Metastable de-excitation spectroscopy and scanning tunneling microscopy study of the 2×4 and 2×7 reconstructions of Ho on Si(001)

Andrew Pratt, Charles Woffinden, Christopher Bonet, and Steve Tear*
Department of Physics, University of York, York YO10 5DD, United Kingdom
(Received 12 May 2008; revised manuscript received 30 September 2008; published 27 October 2008)

Ho silicide nanostructures were formed by the deposition of submonolayer coverages of Ho onto a clean Si(001) 2×1 surface at various substrate temperatures. Depending on the deposition temperature and coverage, the substrate surrounding the nanostructures reconstructs into either a 2×4 or 2×7 structure or a combination of the two. We use metastable de-excitation spectroscopy (He 2^3S) to complement scanning tunneling microscopy (STM) to study these reconstructions revealing the electronic similarities between the 2×4 and 2×7 phases. The presence in the spectra of features due to hybridized Si 3*s*3*p*-Ho 6*s*5*d* bonds at the surface suggest that prominent maxima in the corresponding STM images are due to Ho atoms and that these reconstructions form as a precursor to nanowire formation.

DOI: 10.1103/PhysRevB.78.155430 PACS number(s): 73.20.−r, 73.22.−f, 79.20.Rf

I. INTRODUCTION

For almost a decade now the growth of rare-earth (RE) metal silicides on Si(001) has attracted considerable interest in large part due to the formation of nanowires (NWs) under certain preparation conditions. Aside from potential technological applications such as interconnects for nanoarchitectronics and in optoelectronic and magnetic devices,[1] as quasi-one-dimensional systems NWs possess unique electronic properties that are of interest from a fundamental viewpoint.[2] NWs arise due to an anisotropy in the lattice mismatch of the RE silicide overlayer and the Si(001) substrate, and up to date, NWs of the RE metals Sm,[3] Gd,[4–6] Dy,[7–9] Ho,[9,10] and Er (Refs. 3 and 11–13) have been demonstrated on Si(001) as well as NWs of the chemically similar elements Sc (Ref. 6) and Y.[14] The mismatch for a particular RE determines the lateral dimensions of the NW with typical widths and heights in the ranges of 1–11 nm and 0.2–3 nm, respectively, with lengths extending up to 1 μm.

RE silicide NWs grown on Si(001) have a hexagonal defect-AlB_2 crystal structure with the minimal mismatch between the $[11\bar{2}0]_{RESi_{2-x}}$ and $[1\bar{1}0]_{Si}$ axes resulting in NW growth along this direction, perpendicular to the Si dimer row orientation (see Fig. 1). Along the $[0001]_{RESi_{2-x}}$ direction the strain energy resulting from the greater lattice mismatch to the orthogonal $\langle 110\rangle_{Si}$ axis restricts the width of the NWs, and vacancies in the Si sublattice modify the NW stoichiometry from $RESi_2$ to $RESi_{2-x}$, with $0<x<0.3$. The surface of the NWs is known to reconstruct to give a $c(2\times2)$ structure although a 2×1 reconstruction has also been observed and attributed to the formation of Si dimer bonds.[8] This highlights the strong influence of preparation conditions on NW growth which still requires further understanding. Scanning tunneling spectroscopy measurements have shown that the NWs are indeed metallic,[5,9,10] and more recently, the higher carrier mobility of Ge compared to Si has attracted interest with Ho germanide NWs demonstrated on Ge(001) (Ref. 15) and Ge(111) (Ref. 16) substrates.

The self-assembly of RE silicide nanostructures follows the diffusion-controlled reaction of RE metal adatoms with Si atoms from the substrate with the details of the structure formed determined by the specifics of the growth procedure: predominantly the RE metal coverage, substrate temperature during deposition, and the time and temperature of a post-deposition anneal.[3–13] NWs generally form in the 0.1–0.5 monolayer (ML) coverage range after which islands begin to dominate, becoming more prevalent as the coverage approaches and surpasses 1 ML. The optimum substrate tem-

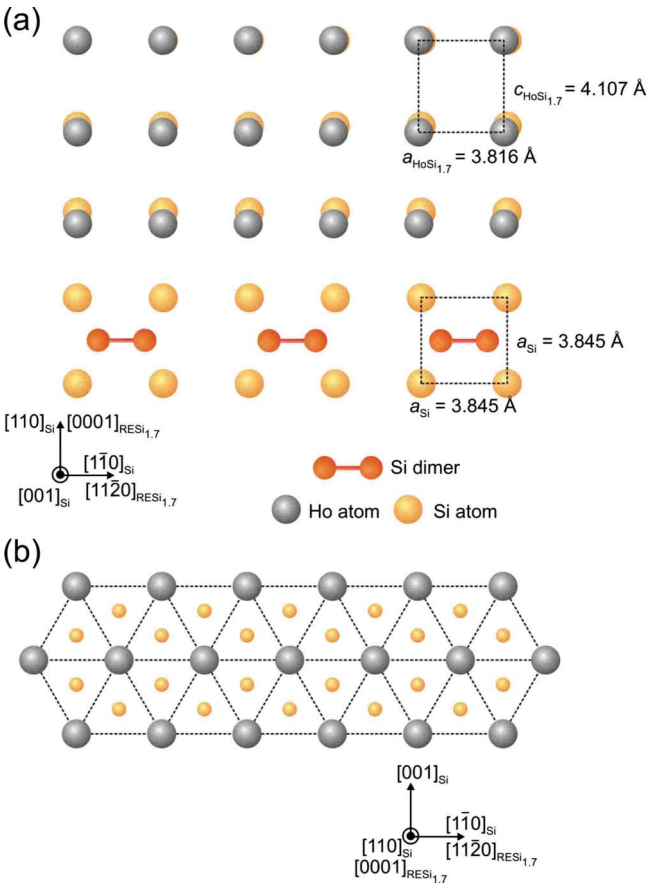

FIG. 1. (Color online) (a) Schematic indicating the NW orientation with respect to Si dimers and the anisotropy in the lattice mismatch of $HoSi_{1.7}$ with the Si(001) surface. (b) Side view of the hexagonal AlB_2 structure of RE silicide NWs.

perature during RE metal deposition for NW growth has been found to be around 600 °C with a postanneal of not more than 5 min.[6] Under these conditions the deposited RE atoms should have fully reacted with the Si substrate. Higher temperatures and longer anneal times yield more islands (at the expense of NWs), as does increased coverage. RE metal coverages of greater than 1 ML on Si(001) have also been investigated recently[13,17] following extensive studies of RE silicide growth on Si(111).[18,19]

RE deposition on Si(001) leads to Stranski-Krastanov growth with nanostructures forming on top of a two-dimensional (2D) wetting layer. Several reconstructions of the substrate surface between the nanostructures have been observed with Yb forming 1×5, 2×3, 2×4, and 2×6 superstructures,[20,21] Er forming 2×3, 5×2, and $c(5\times4)$,[13,22] and Dy,[7,23] Gd,[23] and Ho (Ref. 10) displaying 2×4 and 2×7 reconstructions. Most research on RE metal silicides on Si(001) has concentrated on the formation and structure of NWs and nanoislands with little investigation of the substrate reconstruction separating them. However, understanding this region is important as it acts as a precursor to NW growth and is a potential source of RE metal atoms influencing the dimensions of any nanostructures formed. Ohbuchi and Nogami[10] suggested a model for the 2×4 and 2×7 reconstructions of Ho on Si(001) based on scanning tunneling microscopy (STM) observations although were unable to confirm whether prominent maxima in the STM images were due to Ho atoms rather than a Si-terminated reconstruction with the Ho atoms beneath, as observed for Si(111).[18] This paper makes use of the technique of metastable de-excitation spectroscopy (MDS) to complement STM in the study of the formation of NWs and nanoislands concentrating in particular on the structure of the substrate reconstruction between these features.

In MDS a beam of metastable rare-gas atoms impinges upon a surface to produce an ejected electron energy spectrum that is a characteristic of the surface's electronic, magnetic, and chemical properties. As de-excitation of the metastable atoms is determined by the overlap of surface and atomic wave functions, the technique is extremely surface sensitive and the collected spectra essentially reflect the surface density of states (SDOS). In the case of REs due to orbital overlap, MDS is sensitive to the *s-p* features of the surface valence band which protrude further into the surface vacuum than the more tightly bound $4f$ states. This is in contrast to ultraviolet photoemission spectroscopy (UPS) where surface penetration leads to a less sensitive probe of the surface electronic structure. MDS has been used to investigate RE growth on Si(001) before but only for coverages greater than 1 ML (Refs. 24 and 25) where the surface largely consists of nanoislands. This study investigates sub-ML coverages of Ho on Si(001) with a view to understand the initial stages of the formation of the Ho/Si(001) interface. The ability to probe the surface valence band of a RE overlayer on Si allows information regarding the bonding between the RE atoms and underlying substrate to be garnered, helping to identify the atomic features observed in STM images.

II. EXPERIMENT

STM experiments were performed using an Omicron Nanotechnology GmbH microscope operating at a base pressure of $\sim2\times10^{-10}$ mbar and equipped with low-energy electron diffraction (LEED) capability and a fast-entry lock. Samples were prepared by depositing sub-ML coverages of Ho onto high-ρ *n*-type Si(001) substrates cleaned by flashing several times to 1200 °C for 1 min and followed by heating at 900 °C for 10 min before cooling slowly (<100 °C per minute) to room temperature. Before Ho deposition, LEED was used to check that a sharp 2×1 reconstruction had been obtained and all sample heating was performed by passing a direct current through the sample with the temperature monitored using an infrared (IR) pyrometer. Holmium was deposited from an evaporation source in which the Ho is mounted in a tantalum boat and surrounded by a water-cooled copper shroud. Deposition rates were calibrated using a quartz crystal and were typically less than 0.1 ML per minute (1 ML $=6.78\times10^{14}$ cm^{-2}). During deposition, the Si substrate was held constant at temperatures between 500 and 650 °C with no postanneal after the required coverage had been obtained. Ho coverages of 0.3–0.5 ML were studied with STM and coverages of 0.1, 0.2, 0.3, 0.5, 0.7, 0.9, and 1.0 ML were prepared for MDS experiments. Upon completion of these, to investigate the effects of annealing, some samples were further heated for 5 min at elevated temperatures.

MDS and UPS experiments were carried out in a separate vacuum system to the STM operating at a base pressure of $\sim5\times10^{-10}$ mbar. The MDS apparatus advances conventional methods of MDS by using techniques of laser cooling to produce a high-intensity high-purity beam of He 2^3S atoms and has previously been described in detail.[26] Briefly, He 2^3S atoms, produced in a hollow cold-cathode dc discharge source, supersonically expand into a collimation chamber where resonant laser-light forces collimate the atomic trajectories parallel to the beamline axis. After collimation the atoms enter a separately pumped surface analysis chamber equipped with LEED and Auger electron spectroscopy (AES) and strike a sample inclined at an angle of 45° with respect to the beam and with an intensity of the order of 10^{12} atom s^{-1} cm^{-2}. As unwanted particles in the beam (UV photons and singlet 2^1S He atoms) do not interact with the collimating lasers, their intensity at the sample is negligible. For UPS experiments He I resonance photons ($h\nu=21.22$ eV) from a pure He gas discharge were again incident at 45° to the sample surface. The ejected electron energy spectra resulting from He 2^3S atom or He I photon interaction with the sample surface were measured at normal emission with an Omicron Vakuumphysik GmbH EA 125 hemispherical electron analyzer. A separate but identical Ho source to the one used in the STM experiments was used to deposit Ho onto clean Si(001) with all other preparation conditions remaining the same. Experience has shown that reusing the same Si(001) substrate for different Ho coverages results in MDS spectra and STM images of reduced quality, possibly as a result of the incomplete removal of Ho atoms upon recleaning, and so a fresh Si(001) sample was used for each experiment.

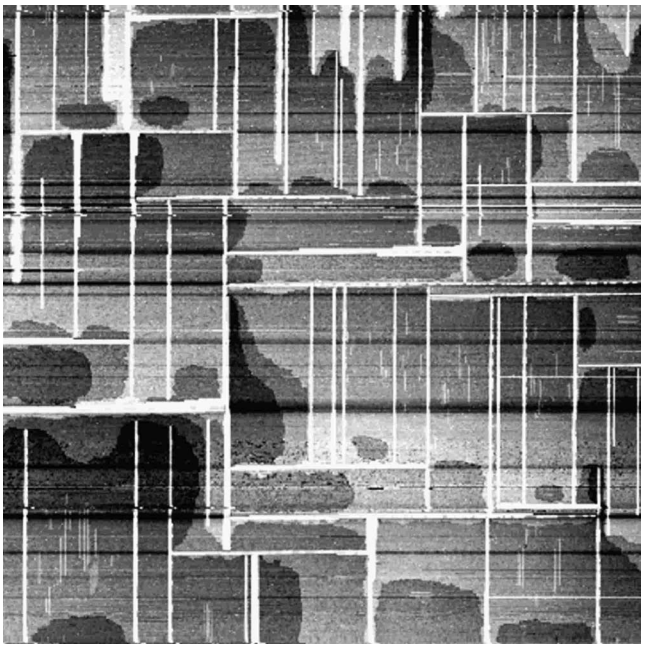

FIG. 2. STM image of NWs formed after the deposition of 0.3 ML of Ho onto a clean Si(001) surface held at 530 °C (700 $\times$700 nm^2, 2.0 V, and 2.0 nA).

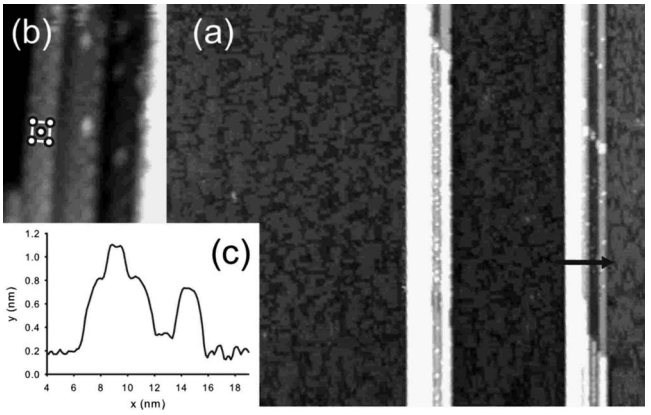

FIG. 3. NWs formed after the deposition of 0.3 ML of Ho with the Si(001) substrate at 610 °C. (a) Between the NWs the reaction of Ho with the substrate results in a partially reconstructed surface (70$\times$75 nm^2,−2.0 V,2.0 nA). NWs are terminated by a $c(2\times2)$ reconstruction which can be distinguished in (b), while second layer NW growth may occur as seen in the line scan of (c), taken from the region of (a) marked with an arrow.

III. RESULTS

A. STM

Figure 2 shows an STM image resulting from the deposition of 0.3 ML of Ho onto a clean Si(001) substrate held at 530 °C during deposition with no postanneal. The NWs formed have thicknesses in the range of 1.5–5.3 nm and lengths of up to 300 nm. Termination of a NW occurs when it is intersected by a perpendicularly growing NW or, less frequently, by the bunching of adjacent Si step edges. During growth, strong reordering of the Si terraces takes place to accommodate the growing NW; with the step edges retreating as Si atoms they, which as their bonding is unsaturated are kinetically more likely to react with the depositing Ho, are donated to the silicide. It follows that NWs also nucleate at step edges. Growth then occurs in a direction perpendicular to the $[1\bar{1}0]$ Si dimer row direction aligning along an orthogonal Si$\langle 110\rangle$ axis. The most common width of NWs in Fig. 2 is 5.3 nm which roughly corresponds to the upper limit imposed by the 6.8% lattice mismatch between the Ho silicide c axis and the underlying Si substrate (a_{Si} =0.3845 nm) so that a NW may accommodate 14 Ho atoms before the strain energy (which in this case is compressive) prevents further widening. Quite frequently though NWs bundle together separated by a strain-relieving trench of one Si dimer width.[5]

The reconstruction of the surface between the NWs depends largely on the quantity of Ho deposited and the substrate temperature during deposition. The increased mobility of Ho atoms associated with elevated substrate temperatures promotes diffusion across the surface favoring nanostructure formation at the expense of substrate reconstruction. Even at high coverages (>1 ML) areas of clean Si may still remain so that the growth mode in these preparation conditions is best described as a combination of Stranski-Krastanov and Volmer-Weber. The partial reconstruction of the Si(001) surface after the deposition of 0.3 ML of Ho at a substrate temperature of 610 °C can be seen in Fig. 3. RE silicide NWs (and nanoislands) are known to be terminated by a $c(2\times2)$ reconstruction,[5] and this can be distinguished in Fig. 3(b) which shows a higher-resolution image of one of the NWs. Quite frequently second layer growth on the NWs occurs and this is evident in Fig. 3(c). A more detailed view of the partially reconstructed surface between the NWs can be seen in Fig. 4. Rows of Si dimers aligned along the Si $[1\bar{1}0]$ direction are disrupted by the appearance of two new types of maxima, one brighter than the other. These maxima appear in subunits consisting of either two bright maxima with a weaker one in between (type A) or a bright maxima surrounded by two that are dimmer (type B), as outlined in the inset. Type A and type B subunits alternate along the direction of the Si dimer rows separated by a dimer vacancy although as the surface is largely unreacted this alternation is not always complete and both type A and type B subunits often appear alone. This lack of long-range order results in a 2×4 LEED pattern for this surface [Fig. 5(b)] although if the reaction of the surface were more complete the true order of this phase would have a 2×8 periodicity. As both type A and type B subunits are clearly related, consisting of three distinct maxima separated by a dimer vacancy, this reconstruction will henceforth be referred to as 2×4, finding consistency with previous studies of this surface.[10,27]

If the deposition temperature is reduced from the generally accepted optimum NW growth temperature of 600 °C then a more complete reconstruction of the surface occurs with more Si dimers being replaced by deposited Ho atoms. Figure 6 shows a filled-state image of the surface resulting from the deposition of 0.3 ML of Ho with the substrate at a temperature of 550 °C. There are no NWs evident in the region of the surface shown which is heavily stepped with

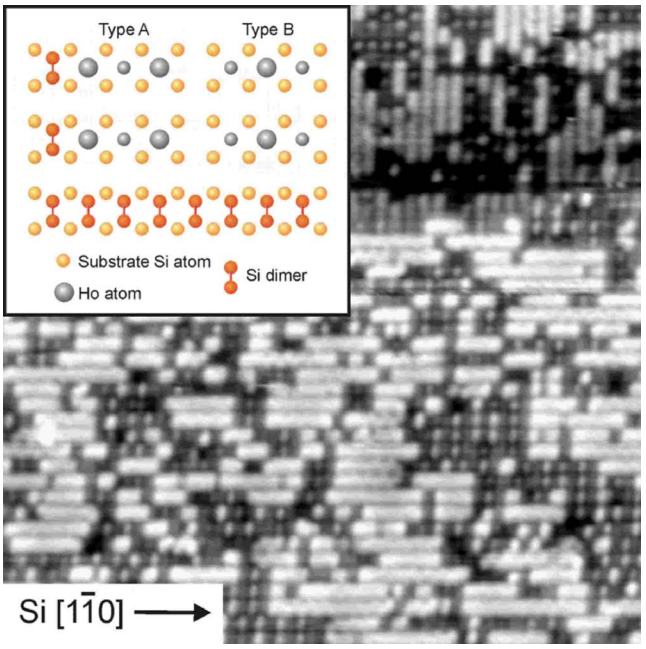

FIG. 4. (Color online) A more detailed image of two terraces of the partially reconstructed surface of Fig. 3. Ho reaction with the substrate interrupts the Si dimer rows to form three-maxima subunits in which individual features alternate in intensity. The inset shows the model proposed by Liu and Nogami (Ref. 27) (30×30 nm^2, -2.0 V, 2.0 nA).

distinctive bright rows aligned along the Si [1$\bar{1}$0] direction that is rotated by 90° on adjacent terraces. Previous work has shown these bright lines to be a distinctive feature of a 2×7 reconstruction,[10,23] which is shown in more detail in the empty- and filled-state images of Fig. 7. Both of these images are from the same area of the surface and are flanked on either side by a brightly appearing NW with periodic features between. In the filled-state image [Fig. 7(a)] these features comprise rows of oblong-shaped maxima interspersed with three-maxima subunits the center of which is brighter than the adjacent two, similar to the type A subunit observed for the 2×4 reconstruction. The 2×7 unit cell is indicated in the figure along with a line that highlights a frequently observed 1a translation in the alignment of subunits. This shift gives rise to antiphase disorder so that the LEED pattern [Fig. 5(c)] displays 1×7 periodicity with streaking along the $\times2$ direction. Alternation of the two types of row present on the 2×7 surface is also evident in the empty-state image [Fig. 7(b)] except that the oblong-shaped maxima distinguishable in the filled-state image now appear as solid bright rows with only two-maxima visible between. The central bright maxima of the subunits observed in the filled-state image have completely disappeared. Liu and Nogami conducted a thorough investigation of the bias dependence of the 2×4 and 2×7 reconstructions for Dy and Gd on Si(001) suggesting that the two types of maxima observed for the 2×4 structure are due to buckling of surface atoms to relieve strain.[23] As more Ho is deposited strain in the 2×4 reconstruction can be further reduced by incorporating the two-maxima bright rows seen in Fig. 7 into the structure. Thus the major difference between the two reconstructions is

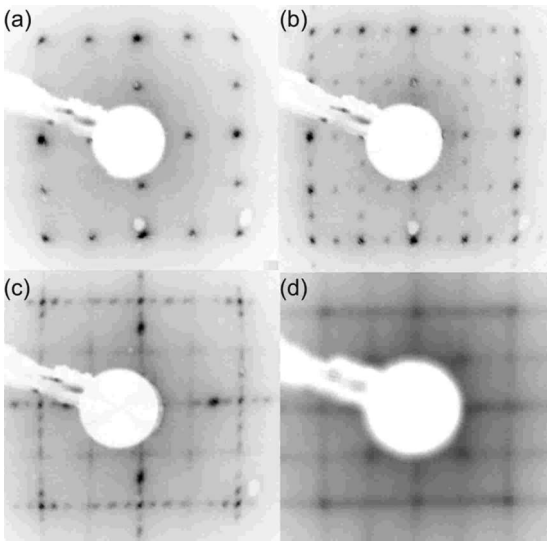

FIG. 5. LEED images from various coverages of Ho deposited onto a clean Si(001) 2×1 surface at 500 °C (beam energy =52 eV). (a) Clean Si(001) 2×1. (b) 0.3 ML of Ho yielding a 2×4 LEED pattern. (c) Deposition of 0.5 ML of Ho. (d) At 1.0 ML coverage the LEED pattern is diffused although some evidence of $c(2\times2)$ is apparent.

FIG. 6. A filled-state image of the 2×7 Ho reconstructed Si(001) surface with 0.3 ML of Ho deposited onto a substrate held at 550 °C (50×20 nm^2, -2.0 V, 2.0 nA).

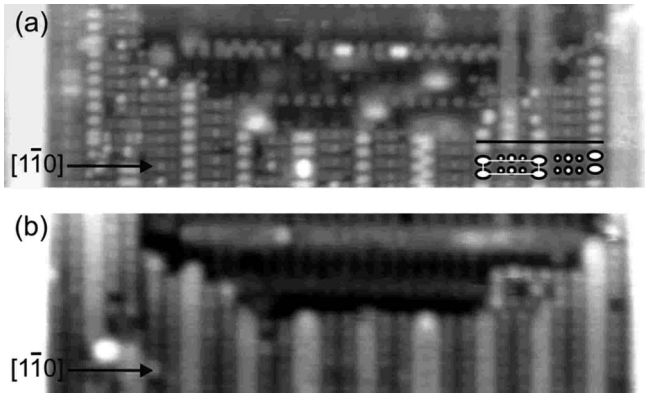

FIG. 7. Detailed (a) filled-state (-2.0 V) and (b) empty-state (2.0 V) images of the 2×7 reconstruction. 0.4 ML of Ho was deposited with the substrate at 575 °C (both images: 29×12 nm^2 and 2.0 nA). The 2×7 unit cell is indicated in (a).

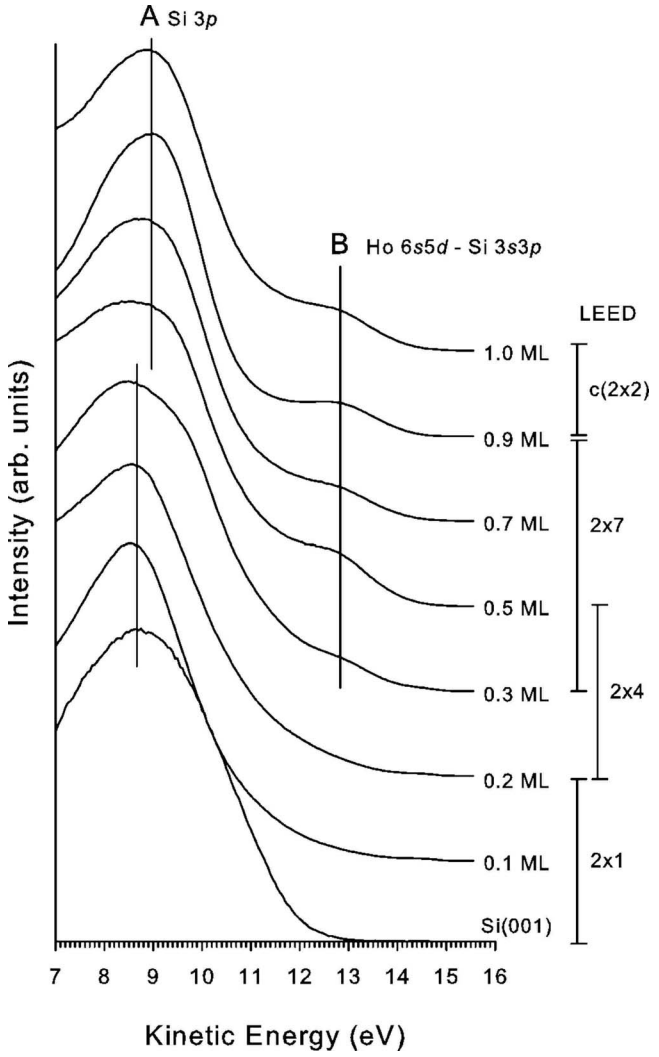

FIG. 8. The MDS spectra for a clean Si(001) 2×1 surface and for sub-ML coverages of Ho deposited with the substrate at a temperature of 500 °C. The coverage dependence of the LEED patterns are shown alongside the MDS spectra.

this feature which appears in the 2×7 phase but not in the 2×4. This also concurs with the observation that the 2×7 only appears at coverages where the 2×4 has already formed and not before.

B. MDS

MDS was performed on samples that had been prepared in the same manner as for the STM experiments described above. Figure 8 shows the MDS spectra obtained from surfaces of Si(001) with varying amounts of Ho deposited onto them with the substrate held at a temperature of 500 °C during deposition and no postanneal. Although it is well established that the optimum temperature for NW formation is around 600 °C, depositing at this lower temperature limits Ho mobility, and therefore the formation of nanostructures while allowing the complete reaction of the depositing metal with the substrate. The quality of the resulting reconstructed surfaces was verified using LEED before MDS experiments commenced. Also shown in Fig. 8 for comparison is the spectrum that results from a clean Si(001) 2×1 surface. It is well established that when incident on semiconducting surfaces He 2^3S atoms are resonantly ionized with the excited $2s$ electron of the He atom tunneling into an empty state of the surface. This is followed by Auger neutralization (AN) where the He^+ ion formed in the resonant ionization (RI) process is neutralized in a core-valence-valence-type Auger transition.[28] An alternative de-excitation mechanism for metastable atoms at solid surfaces is Auger de-excitation (AD), which as a one-electron process, where an electron from the surface tunnels into the He $1s$ ground state with the simultaneous release of the He $2s$ electron, is more reminiscent of photoemission resulting in spectra that are generally easier to interpret than for RI+AN. This process usually occurs at insulating surfaces and at semiconducting/conducting surfaces with a particularly low work function. In both cases the electron emission spectrum arises from interaction between the He 2^3S beam and the surface orbitals which protrude furthest into the vacuum rendering MDS an extremely sensitive probe of the SDOS. However, as RI+AN is a two-electron process the spectra resulting from surfaces at which this de-excitation channel is predominant are generally broad and featureless as distinct bands present in the SDOS are self-convoluted in the corresponding MDS spectrum. These characteristics are observed in the spectrum for the clean Si(001) 2×1 surface confirming that He 2^3S de-excitation is through the RI+AN process with no evidence of emission due to the surface state arising from the dangling bond located on the dimer row of the 2×1 reconstruction, as observed in UPS (see below). The contribution of this surface state, which would be expected to be seen in the high kinetic-energy region, to the MDS spectrum overlaps with emission from the bulk. Si $3p$ states that are present both at the surface and in the bulk account for the overall shape of the spectrum,[29] which peaks at a kinetic energy of approximately 8.7 eV (labeled A in Fig. 8). Emission at lower energies is dominated by secondary electrons although features arising from surface valence bands would not be expected to appear here. The high kinetic-energy cutoff of the MDS spectrum occurs at 13.2 ± 0.2 eV agreeing with previous results.[24,29]

The MDS spectra obtained for various coverages of Ho on Si(001) have several notable differences to the clean Si(001) 2×1 spectrum. As the coverage approaches 0.3 ML the emission observed at high kinetic energies (>12 eV) gradually increases indicating that a significant portion of the He 2^3S beam is now de-exciting through the AD process. However, at these low coverages large areas of unreacted Si(001) 2×1 remain on the surface, as confirmed by STM and LEED, so that the local de-excitation channel at these regions is still RI+AN. The resulting spectrum then arises due to electron emission originating from both AD and RI+AN. For 0.3 ML the LEED pattern displayed a 2×4 structure and the emission at high kinetic energies has evolved into a distinctive feature centered around 12.8 eV (labeled B) indicating the continued reaction of the Si substrate with the deposited Ho so that AD now dominates. As the coverage increases feature B remains approximately constant in position and intensity, while the corresponding LEED patterns

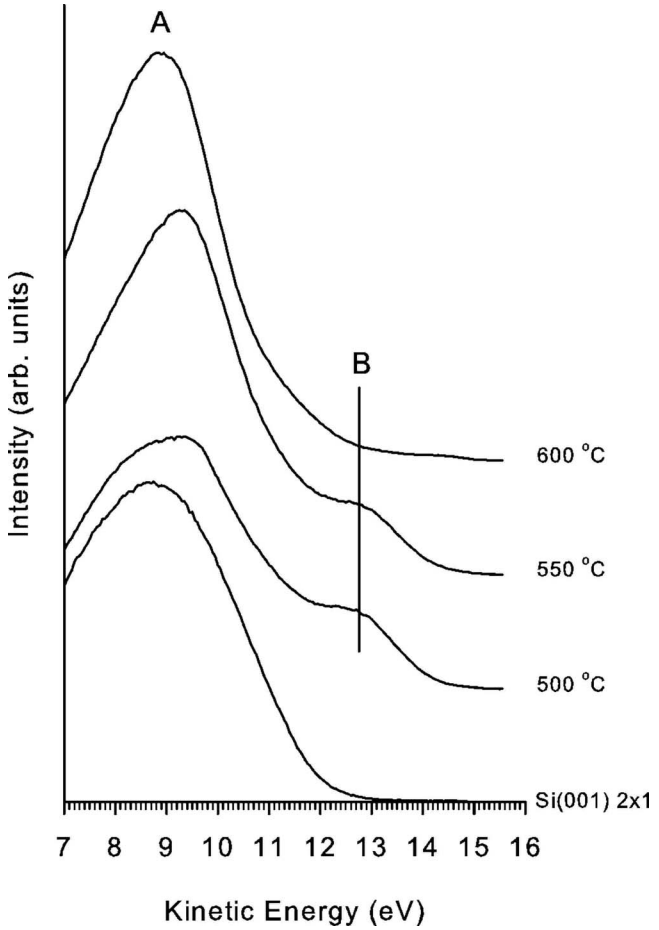

FIG. 9. MDS spectra as a function of anneal temperature for a Ho coverage of 0.7 ML.

showed that the surface order had evolved from a 2×4 to a 2×7 reconstruction which was sharpest at 0.7 ML before becoming less distinguishable at 0.9 and 1.0 ML [see Fig. 5(d)]. As well as the emergence of feature B as the Ho coverage increases, the position and form of feature A corresponding to emission from Si $3p$ states also evolves. The peak, centered at a value of around 8.7 eV for the clean surface, remains approximately constant until at 0.3 ML a shoulder on the peak begins to appear. As the coverage increases this feature results in peak A shifting to a higher kinetic energy, reaching a maximum of approximately 9.0 eV. This behavior again correlates to the observed changes in the corresponding LEED patterns described above.

Previous studies of RE NW systems have shown how sensitive NW growth is to the specific preparation conditions, particularly with regard to the substrate temperature during deposition. Figure 9 shows how 0.7 ML of Ho deposited onto a clean Si(001) 2×1 surface at 500 °C responds to further annealing. To produce these results, after deposition at 500 °C the surface was left to cool to room temperature before LEED and MDS were carried out. The sample was then annealed for 5 min at first to 550 °C and then to 600 °C, in each case waiting for the sample to cool again to RT before LEED and MDS were performed. At the deposition temperature of 500 °C a sharp 2×7 LEED pattern was obtained and the form of the MDS spectrum is similar to that observed in Fig. 8 with a shift in the peak position of feature A and also the presence of feature B. Annealing at 550 °C for 5 min appears to sharpen these features and the corresponding LEED pattern was predominantly 2×4 in nature. After a 600 °C anneal, emission at high kinetic energies has strongly reduced so that feature B is no longer present and the shape of the spectrum resembles that of the clean Si(001) 2×1 surface although narrower. LEED also indicated that a 2×1 surface had been recovered. On the whole, the dependence of the electron emission spectrum on anneal temperature and anneal time for the different Ho coverages investigated repeated the trend observed in Fig. 9; however the lower the coverage, the lower the anneal time is needed for the signature of a clean Si(001) 2×1 surface to appear in LEED and MDS.

IV. DISCUSSION

STM has shown that, when 0.3–0.5 ML of Ho is deposited onto a Si(001) substrate, the surface surrounding the NWs formed reconstructs into either a 2×4 or 2×7 phase, with the specific phase determined mainly by the deposition temperature and coverage. Below around 0.3 ML, areas of clean Si(001) 2×1 remain, coexisting with the 2×4 reconstruction. 0.3 ML appears to be an approximate coverage above which a transition in the surface reconstruction to a 2×7 phase occurs, as observed in both LEED and STM. As the coverage approaches 1 ML the increase in the NW and nanoisland density is accompanied by disorder in the corresponding LEED pattern although some evidence of the 2×7 phase remains. Due to the change in Ho mobility at different substrate temperatures, the NW density may vary along with the amount of Ho available for surface reconstruction. A higher deposition temperature favors nanostructure formation thereby increasing the overall coverage at which the 2×7 phase becomes predominant in reconstructed areas. Annealing at high temperatures appears to reverse the progression of the surface ordering to yield large areas of clean Si(001) 2×1 even at high coverages. This suggests that Ho atoms consumed during the formation of the 2×4 and 2×7 reconstructions at low anneal temperatures can gain enough mobility when heated further to break free of the reconstruction and join the growing nanostructures. Such an observation is consistent with photoemission studies of the Er/Si(001) interface which showed that the presence of Si dimers on the surface remained approximately constant for Er coverages of 2–8 ML.[30]

Given that both the 2×4 and 2×7 phases include similar three-maxima subunits with the latter phase also consisting of bright rows of maxima of two atoms, the question arises as to what the identity of the atoms giving rise to these features is. A model proposed by Liu and Nogami[27] for the 2×4 reconstruction of Dy on Si(001) assumes each maximum to be due to the replacement of a Si dimer with a single Dy atom. Each unit cell of an ideally reconstructed 2×4 surface would then contain three atoms to yield a Ho coverage of 3/8 or 0.375 ML agreeing with measurements of the nominal coverage. A similar argument for the Gd 2×7 puts the metal content for this reconstruction at 5/14 or 0.357 ML,

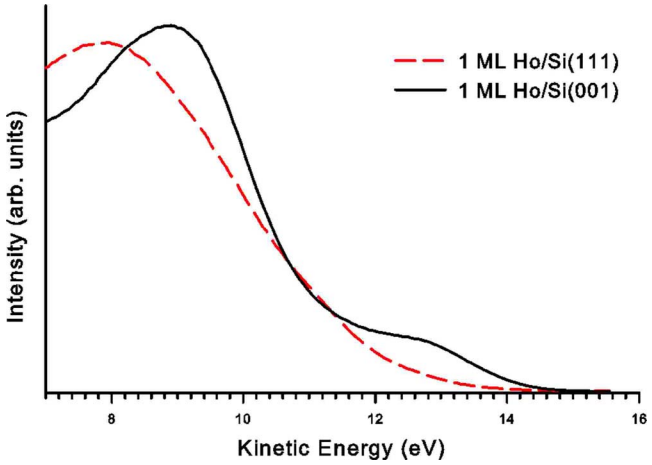

FIG. 10. (Color online) A comparison of 1 ML of Ho deposited onto clean Si(001) and Si(111) substrates.

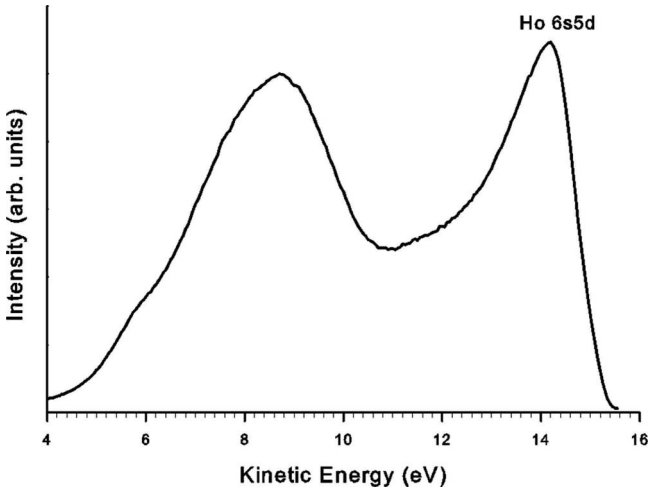

FIG. 11. The MDS spectrum from 6 ML of Ho deposited onto a clean Si(001) 2×1 surface with the substrate at room temperature.

again agreeing with observations.[23] This suggests that the assumption of one RE atom per STM maximum is a reasonable one although a similar study of the Ho content of the 2×4 phase yields 1.5 Ho atoms per unit cell with only one of the two types of maxima observed in this structure being due to the RE.[10] With STM and LEED alone it is difficult to eliminate the possibility that the maxima observed in STM images of the 2×4 and 2×7 phases (see Figs. 4 and 7) are not due to RE atoms at all but are instead due to Si atoms sitting atop a subsurface RE layer. Such a situation finds comparison in the case for RE deposition on Si(111) where the threefold symmetry of the substrate leads to the formation of 2D silicide films with a 1×1 reconstruction consisting of a ML of RE atoms subsurface to a reverse-buckled Si bilayer.[18] Figure 10 shows how the MDS spectrum for 1 ML of Ho deposited onto a clean Si(001) sample compares to that for a 2D RE silicide formed on Si(111) when 1 ML of Ho is deposited onto a room temperature Si(111)-7×7 surface, followed by an anneal at 500 °C for 10 min. The featureless form of the Ho/Si(111) spectrum would be expected from a surface where the de-excitation mechanism is RI +AN as occurs on the top Si layer of the 2D silicide. The increased emission at high kinetic energies giving rise to the feature centered around 12.8 eV for the Ho/Si(001) surface suggests that in this case a Si bilayer does not form.

As for LEED and STM, a Ho coverage of 0.3 ML also appears to be a threshold in the MDS spectra of Fig. 8. It is above this coverage that the peak position of feature A begins to shift to higher kinetic energies and also the coverage at which feature B first becomes prominent. Feature A is attributed to emission from Si $3p$ states present in the clean Si(001) 2×1 surface but also in the Ho reconstructed phases and the Ho silicide of the NWs and nanoislands. A photoemission study of the Er/Si(001) interface indicates that band bending due to the silicide formation induces a Si-core level shift which is maximum at an Er coverage of 0.6 ML.[30] A binding energy shift of ~0.3 eV for both Si $2p$ and $3p$ valence features was reported which agrees well with our measured maximum displacement of the Si $3p$ peak.

Feature B is attributed to bonding between hybridized Si $3s3p$ states and hybridized Ho $5d6s$ states in the silicide as remarked for higher coverage MDS studies of Er and Yb on Si(001) (Ref. 25) and for the UPS study of Er on Si(001).[30] Further evidence for this assignment comes from comparison to the Ba/Si(001) system which shows a similar feature.[31] These similarities and the fact that Ba, although electronically similar to the REs, does not contain any $4f$ electrons, strengthens the assertion that the He 2^3S interaction with RE $4f$ states is negligible. The assignment of feature B as being due to hybridized Si $3s3p$ and Ho $5d6s$ states is also supported by partial DOS calculations for Er silicide.[32]

Due to the lack of emission observed in the MDS spectra around E_F it has been proposed that the RE/Si(001) interface is semimetallic.[33] Figure 11 shows the MDS spectrum from 6 ML of Ho deposited onto a clean Si(001) substrate at room temperature. Strong emission is observed just below E_F due to the $6s5d$ state in the deposited Ho,[24] which indicates that very limited reaction with the substrate has taken place. When deposited at an elevated substrate temperature MDS has shown that these Ho $6s5d$ states bond with Si $3s3p$ hybridized states to yield the RE silicide that gives rise to feature B in the MDS spectra. As this bonding occurs charge is transferred from Ho to Si resulting in a surface dipole effect that significantly lowers the surface work function.[28] Through the dynamics of He 2^3S interaction with the surface the de-excitation mechanism then changes from RI+AN to AD, as observed in the MDS spectra. AD will proceed if the lowering of the work function prevents the $2s$ electron of the He 2^3S atom from tunneling into an empty state of the metal/semiconducting surface thus suppressing the RI process. As AD is a one-electron process similar to photoemission, electron emission occurs up to the excitation energy of the He 2^3S atom. This can be measured from the kinetic-energy cutoff which reaches a maximum value of 15.3 ± 0.2 eV for a coverage of 0.5 ML. Together with the analyzer work function of 4.45 eV, this yields an estimate of the effective excitation energy for the He 2^3S $2s$ level of 19.75 ± 0.2 eV which agrees with the gas-phase value of 19.82 eV, not showing any significant deviation due to the image force effect.

By considering the MDS results obtained by ourselves for the sub-ML deposition of RE on Si(001) and by others for coverages greater than 1 ML (Refs. 24 and 25) and by comparing these to STM and LEED studies, a clear picture emerges of the evolution of silicide formation at the RE/Si(001) interface. Initially, deposited RE atoms react with the clean Si(001) 2×1 substrate to yield a partially reconstructed 2×4 surface which progresses to form a 2×7 ordered phase as the amount of Ho deposited increases. As the coverage approaches 1 ML, NWs and nanoislands become more prevalent, coexisting with areas of reconstructed and also clean substrate. The MDS spectra are very similar for all of these stages of interface formation being dominated by a strong peak due to emission from bulklike and silicide Si $3p$ bands and a high kinetic-energy feature arising from hybridized Ho $6s5d$ and Si $3s3p$ states. While before these states have been observed for the silicides formed for high depositions (1–12 ML), their occurrence in this sub-ML study suggests that the 2×7 phase, and hence in turn the 2×4 phase, acts as a precursor to NW formation. Furthermore, this supports models based on metal-atom conservation that distinctive maxima observed in STM topographs of these structures are due to deposited RE rather than Si atoms.[10,23]

The extreme surface sensitivity of MDS and its applicability as a technique to the study of surface electronic structure is highlighted by comparison with UPS studies of Ho reconstructed Si(001). Figure 12 shows He I photoemission spectra obtained at normal emission for a clean Si(001) 2×1 surface and for a range of Ho coverages. The strong surface state at ~0.7 eV below E_F is due to the dangling bond localized on the 2×1 dimer row and disappears after 0.5 ML Ho deposition. A strong feature is present at a binding energy of around 6.5 eV for all Ho coverages as well as the clean surface and is attributed to emission from Si $3p$ states. However due to the increased surface penetration compared to MDS evidence for bonding between Si $3s3p$ and Ho $6s5d$ states is not clear.

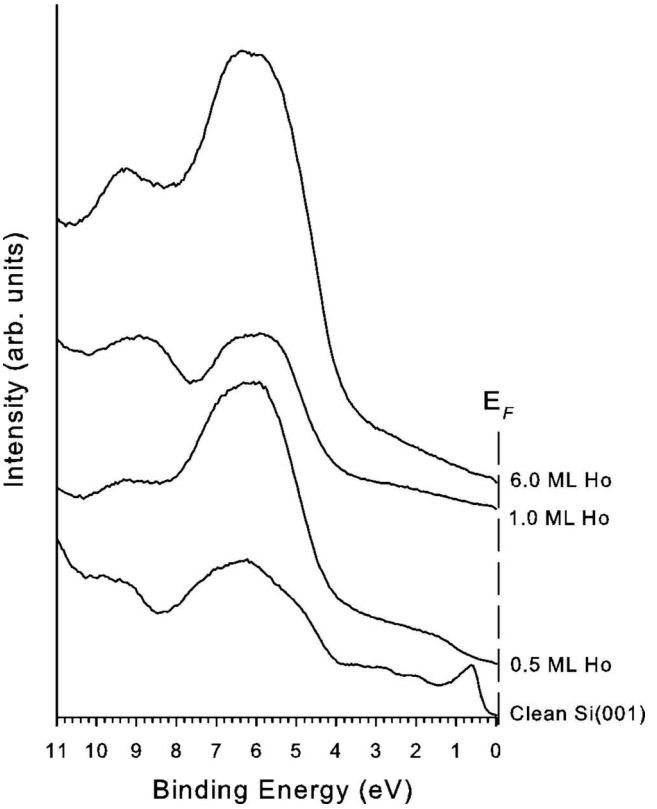

FIG. 12. Normal emission He I ($h\nu$=21.22 eV) UPS spectra for clean and Ho-reconstructed Si(001).

V. CONCLUSIONS

Using MDS we have investigated sub-ML coverages of Ho on Si(001) and the nature of the interface formed, in particular the specific features of the surface which give rise to prominent maxima in corresponding STM images and to distinctive 2×4 and 2×7 reconstructions. Similarities in data obtained for the two phases and comparison of this data to higher coverage studies[24] indicates that these reconstructions form as a precursor to NW growth suggesting that the assumption that the STM maxima are due to Ho atoms at the surface is somewhat justified and supports previously suggested models for the structure of these phases.[10,23] Further studies are required to determine a more detailed structural model for the 2×4 and 2×7 reconstructions. One potential technique that could achieve this is LEED $I(V)$ analysis although to be successful large uninterrupted domains of both phases would be required. *Ab initio* calculations would also greatly benefit here. Both approaches are helped by a reasonably accurate starting model to obtain good agreement between theory and experiment, and the analysis presented here will contribute to the deduction of such a model.

ACKNOWLEDGMENTS

We would like to acknowledge the U.K. Engineering and Physical Sciences Research Council for funding this project.

*spt1@york.ac.uk

[1] D. R. Bowler, J. Phys.: Condens. Matter **16**, R721 (2004).
[2] H. W. Yeom, S. Takeda, E. Rotenburg, I. Matsuda, K. Horikoshi, J. Schaefer, C. M. Lee, S. D. Kevan, T. Ohta, T. Nagao, and S. Hasegawa, Phys. Rev. Lett. **82**, 4898 (1999).
[3] R. Ragan, Y. Chen, D. A. A. Ohlberg, G. Medeiros-Ribeiro, and R. S. Williams, J. Cryst. Growth **251**, 657 (2003).
[4] B. Z. Liu and J. Nogami, Nanotechnology **14**, 873 (2003).
[5] D. Lee and S. Kim, Appl. Phys. Lett. **82**, 2619 (2003).
[6] Y. Chen, D. A. A. Ohlberg, and R. S. Williams, J. Appl. Phys. **91**, 3213 (2002).
[7] B. Z. Liu and J. Nogami, J. Appl. Phys. **93**, 593 (2003).

[8] C. Preinesberger, S. K. Becker, S. Vandré, T. Kalka, and M. Dähne, J. Appl. Phys. **91**, 1695 (2002).
[9] J. Nogami, B. Z. Liu, M. V. Katkov, C. Ohbuchi, and N. O. Birge, Phys. Rev. B **63**, 233305 (2001).
[10] C. Ohbuchi and J. Nogami, Phys. Rev. B **66**, 165323 (2002).
[11] Y. Chen, D. A. A. Ohlberg, G. Medeiros-Ribeiro, Y. A. Chang, and R. S. Williams, Appl. Phys. Lett. **76**, 4004 (2000).
[12] Y. Chen, D. A. A. Ohlberg, and R. S. Williams, Mater. Sci. Eng., B **87**, 222 (2001).
[13] Y. Zhu, W. Zhou, S. Wang, T. Ji, X. Hou, and Q. Cai, J. Appl. Phys. **100**, 114312 (2006).
[14] M. Katkov and J. Nogami, Bull. Am. Phys. Soc. **47**, 283 (2002).
[15] C. Bonet and S. P. Tear, Appl. Phys. Lett. **89**, 203119 (2006).
[16] C. Eames, C. Bonet, M. I. J. Probert, S. P. Tear, and E. W. Perkins, Phys. Rev. B **74**, 193318 (2006).
[17] T. J. Wood, C. Eames, C. Bonet, M. B. Reakes, T. C. Q. Noakes, P. Bailey, and S. P. Tear, Phys. Rev. B **78**, 035423 (2008).
[18] C. Bonet, I. M. Scott, D. J. Spence, T. J. Wood, T. C. Q. Noakes, P. Bailey, and S. P. Tear, Phys. Rev. B **72**, 165407 (2005).
[19] E. W. Perkins, C. Bonet, and S. P. Tear, Phys. Rev. B **72**, 195406 (2005).
[20] M. Kuzmin, P. Laukkanen, R. E. Perälä, R. L. Vaara, and I. J. Väyrynen, Appl. Surf. Sci. **222**, 394 (2004).
[21] M. V. Katkov and J. Nogami, Surf. Sci. **524**, 129 (2003).
[22] Q. Cai, J. Yang, Y. Fu, Y. Wang, and X. Wang, Appl. Surf. Sci. **190**, 157 (2002).
[23] B. Z. Liu and J. Nogami, Surf. Sci. **540**, 136 (2003).
[24] L. Pasquali, S. D'Addato, and S. Nannarone, Phys. Rev. B **65**, 115417 (2002).
[25] L. Pasquali and S. Nannarone, Nucl. Instrum. Methods Phys. Res. B **230**, 340 (2005).
[26] A. Pratt, A. Roskoss, H. Ménard, and M. Jacka, Rev. Sci. Instrum. **76**, 053102 (2005).
[27] B. Z. Liu and J. Nogami, Surf. Sci. **488**, 399 (2001).
[28] Y. Harada, S. Masuda, and H. Ozaki, Chem. Rev. (Washington, D.C.) **97**, 1897 (1997).
[29] S. Masuda, H. Ishii, and Y. Harada, Surf. Sci. **242**, 400 (1991).
[30] G. Chen, X. Ding, Z. Li, and X. Wang, J. Phys.: Condens. Matter **14**, 10075 (2002).
[31] S. Hongo, K. Ojima, S. Taniguchi, T. Urano, and T. Kanaji, Appl. Surf. Sci. **82-83**, 537 (1994).
[32] L. Magaud, J. Y. Veuillen, D. Lollman, T. A. Nguyen Tan, D. A. Papaconstantopoulos, and M. J. Mehl, Phys. Rev. B **46**, 1299 (1992).
[33] R. Hofmann, W. A. Henle, F. P. Netzer, and M. Neuber, Phys. Rev. B **46**, 3857 (1992).